Journal of Sedimentary Research, 2024, v. 94, 527–540
1st Bouma Special Publication
DOI: 10.2110/jsr.2024.012

THE ROLE OF BOTTOM MESO-SCALE DYNAMICS IN CONTOURITE FORMATION IN THE ARGENTINE BASIN

GASTÓN KREPS,[1,2] TILMANN SCHWENK,[3,4] SILVIA ROMERO,[2,5,6] AGUSTÍN QUESADA,[7,8] JENS GRUETZNER,[1] VOLKHARD SPIESS,[3,4] HANNO KEIL,[3,4] RUBEN KANTNER,[3] LESTER LEMBKE-JENE,[1] RAMIRO FERRARI,[9] FRANK LAMY,[1] AND ELDA MIRAMONTES[3,4]

[1]*Alfred-Wegener-Institut Helmholtz-Zentrum für Polar-und Meeresforschung, Bremerhaven, Germany*
[2]*Departamento de Ciencias de la Atmósfera y de los Océanos, Facultad de Ciencias Exactas y Naturales, Universidad de Buenos Aires, Buenos Aires, Argentina*
[3]*Faculty of Geosciences, University of Bremen, Bremen, Germany*
[4]*MARUM, Center for Marine Environmental Sciences, University of Bremen, Bremen, Germany*
[5]*Departamento Oceanografía, Servicio de Hidrografía Naval, Buenos Aires, Argentina*
[6]*Universidad de la Defensa Nacional, Maipú 262, C1084 ABF, Buenos Aires, Argentina*
[7]*Universidad Nacional de Río Negro, Instituto de Investigaciones en Recursos Naturales, Agroecología y Desarrollo Rural, Río Negro, Argentina*
[8]*Consejo Nacional de Investigaciones Científicas y Técnicas, Instituto de Investigaciones en Recursos Naturales, Agroecología y Desarrollo Rural, Río Negro, Argentina*
[9]*NOVELTIS, 153 Rue du Lac, 31670 Labège, France*
e-mail: gaston.kreps@awi.de

ABSTRACT: **The Argentine Basin is a deep-sea basin located in the South Atlantic Ocean that contains sedimentary deposits derived from different provenances. It is characterized by complex ocean dynamics encompassing diverse spatial and temporal dimensions. The northward subantarctic Malvinas Current and southward subtropical Brazil Current converge at the western margin of the Argentine Basin, resulting in the formation of the Brazil–Malvinas Confluence region. Bottom currents, particularly currents flowing alongslope and horizontal eddies, are crucial in shaping the seafloor and in the formation of sedimentary features (e.g., contourites). The poorly understood strength and variability of bottom currents leave the processes that control sedimentation in deep environments unclear. High-resolution (1/12°) reanalysis was used to analyze near-bottom flows and bottom dynamics were compared with seafloor sedimentary characteristics obtained from geophysical datasets and sediment cores. High speeds, up to 3.5 m/s at the surface and up to 1.4 m/s at the bottom, reveal the presence of intense flows in this area. The Zapiola Drift, an ∼ 1,200 m high sedimentary deposit located in the central part of the Argentine Basin, is bounded by a zone of high bottom eddy kinetic energy (EKE) that resulted in the erosion of the seafloor and in the accumulation of sandy mud. The Malvinas Current is distinguished by strong and constant currents flowing northwards along the continental slope and by minimal EKE at the bottom. The area of the continental slope along which the Malvinas Current flows corresponds to a contourite terrace, a relatively flat surface composed almost entirely of sandy sediments and with abundant erosional features. The regions of highest EKE activity in the bottom layer is the overshoot of the Brazil Current and the abyssal plain. Our study highlights the impact of bottom-current dynamics on contouritic sedimentation. In certain regions, the process of sedimentation is subject to the influence of sporadic events that occur between periods of intense and weak flow. These events are regarded as intermittent processes. While sedimentation in other areas is controlled by constant flows. A better understanding of the strength and variability of bottom currents will improve paleoceanographic reconstructions based on the sedimentary record.**

INTRODUCTION

The South Atlantic Ocean has a distinct function in the global overturning circulation, because it is the sole ocean basin presenting a net heat transport towards the equator (Talley 2003; Garzoli et al. 2013; Trenberth and Zhang 2019; Chidichimo et al. 2023, among others). An important interaction between the upper and abyssal cells of the Atlantic Meridional Overturning Circulation (AMOC) is observed in the South Atlantic Ocean (Chidichimo et al. 2023), contributing significantly to climate change (Kostov et al. 2014; Buckley and Marshall 2016; Pérez et al. 2018).

Contour-following currents driven by the thermohaline circulation have a substantial influence on sedimentation in continental margins and abyssal plains, and sometimes lead to the formation of large-scale deposits or erosional features (Kennett 1983; Stow et al. 2002, 2009; Rebesco and Camerlenghi 2008; Hernández-Molina et al. 2010). Deposits formed by currents flowing near the seafloor (i.e., bottom currents) are classified as contourites (Rebesco and Camerlenghi 2008; Rebesco et al. 2014). In zones with relatively weak currents, muddy contourites tend to accumulate, while in zones with strong currents fine-sediments can be winnowed resulting in the formation of sandy contourites, or they can even be eroded under high-energy conditions (Miramontes et al. 2021).

Published Online: October 2024
 1527-1404/24/094-527

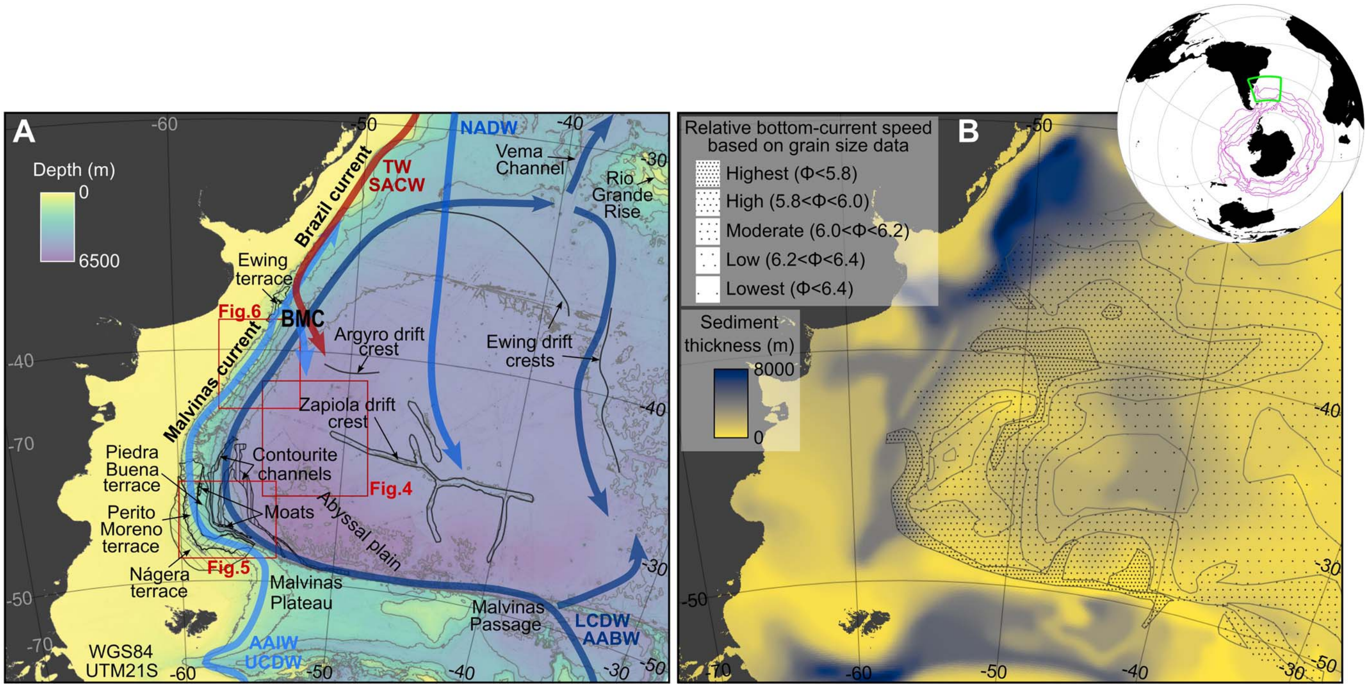

FIG. 1.—**A)** Bathymetric map of the Argentine Basin showing the main contourite features (modified from Ewing and Lonardi 1971; Flood and Shor 1988; Hernández-Molina et al. 2010) and the general circulation pattern (adapted from Stramma and England 1999; Valla et al. 2018). NADW, North Atlantic Deep Water; TW, Tropical Water; SACW, South Atlantic Central Water; AAIW, Antarctic Intermediate Water; UCDW, Upper Circumpolar Deep Water; LCDW, Lower Circumpolar Deep Water; AABW, Antarctic Bottom Water; BMC, Brazil–Malvinas Confluence. The white boxes represent the regions analyzed in more detail in this work. **B)** Total sediment thickness (from Straume et al. 2019) and relative bottom-current speed interpreted from mean silt grain size of surface sediments (from Ledbetter 1986). Note the relatively high sediment thickness (up to about 3000 m.) in the area of the Zapiola Drift in the central part of the basin.

Bottom currents, specifically horizontal eddies, along with topographic features, play a vital role in shaping the seafloor and in formation of contourites (e.g., Miramontes et al. 2021; Wilckens et al. 2021; Kreps et al. 2023). But it still is unclear which specific conditions lead to the mobilization, modification, and deposition of sediments via bottom currents (Miramontes et al. 2019a).

The relationship between sediment and current dynamics can be investigated through the analysis of sediment grain size. Particle size has been linked to the velocity of the corresponding flow responsible for transportation and deposition, as evidenced by Ledbetter and Johnson (1976) and McCave and Swift (1976). Under a specific stress, certain grains and aggregates deposit while others with smaller settling velocity remain in turbulent suspension and are transported farther downstream (McCave et al. 2017). This method of paleoceanographic reconstruction involves selective deposition and removal of finer materials through winnowing, as described by McCave et al. (1995) and McCave and Hall (2006). However, the link between the oceanographic conditions and the resulting deposits is not clear yet; there is no universal relationship between mean sortable silt and mean current speed (McCave et al. 2017), and it is unknown how short-lived, high-energy events imprint the sedimentary record.

The Argentine Basin (AB) is an active deep-sea sedimentary deposit of very intense ocean circulation that strongly controls seafloor morphology, grain size distribution, and the transport and accumulation of organic matter (e.g., Ledbetter 1986; Frenz et al. 2004; Mollenhauer et al. 2006; Hernández-Molina et al. 2010; Wilckens et al. 2021). However, bottom-current circulation is poorly constrained in the area. In this study, in order to better constrain the oceanographic conditions under which different types of contourites form, we analyze the intensity, direction, and variability of bottom currents and compare them with the distribution and characteristics of sedimentary deposits. To achieve this objective, we performed an analysis of 28 years of GLORYS12 reanalysis data and compared the modeled results with observations from hydrographic, bathymetric, hydroacoustic, and seismic data, as well as from sediment cores.

FORMATION AND EVOLUTION OF THE ARGENTINE BASIN

The geological history of the South Atlantic sedimentary basins began with crustal stretching on the western margin of Gondwana during the Permian–Triassic Orogeny. This activity resulted in regional north–south-trending rifts that were subsequently filled with non-marine clastic sediments (Urien and Zambrano 1996; Ramos 1996). The volcanic events associated with this rift system serve as precise indicators for determining the timing of Gondwana's breakup. This breakup created a cavity subsequently occupied by the proto–South Atlantic shallow seas, displaced by transform-fault systems from south to north. The opening phase of the South Atlantic Ocean, marked by the formation of oceanic crust between South America and Africa, began during the Early Cretaceous, about 138 million years ago, from south to north (Pérez-Díaz and Eagles 2014).

Then the South Atlantic Ocean underwent rapid deepening and widening, resulting in the formation of two ocean basins separated by a shallow barrier located at the present-day Walvis Ridge and Rio Grande Rise (Van Andel et al. 1977). The AB (Fig. 1) is the deep-water basin situated south of this barrier, extending over the lower slope and continental-rise region of the Argentinian passive volcanic continental margin. Its sedimentary fill is over 5,000 meters thick, covering an area of approximately 200,000 km^2 in the South West Atlantic Ocean (Fig. 1).

Topographically, the deepest point of the AB is situated along the western and southwestern margins, referred to as the Abyssal Gap, with a maximum water depth of 6,212 meters (Lonardi and Ewing 1971; Ewing and Lonardi 1971; Parker et al. 1996, 1997; Hernández-Molina et al. 2010). Three prominent topographic features associated with contourite drifts in the AB are the Zapiola, Argyro, and Ewing (Fig. 1). These features result from

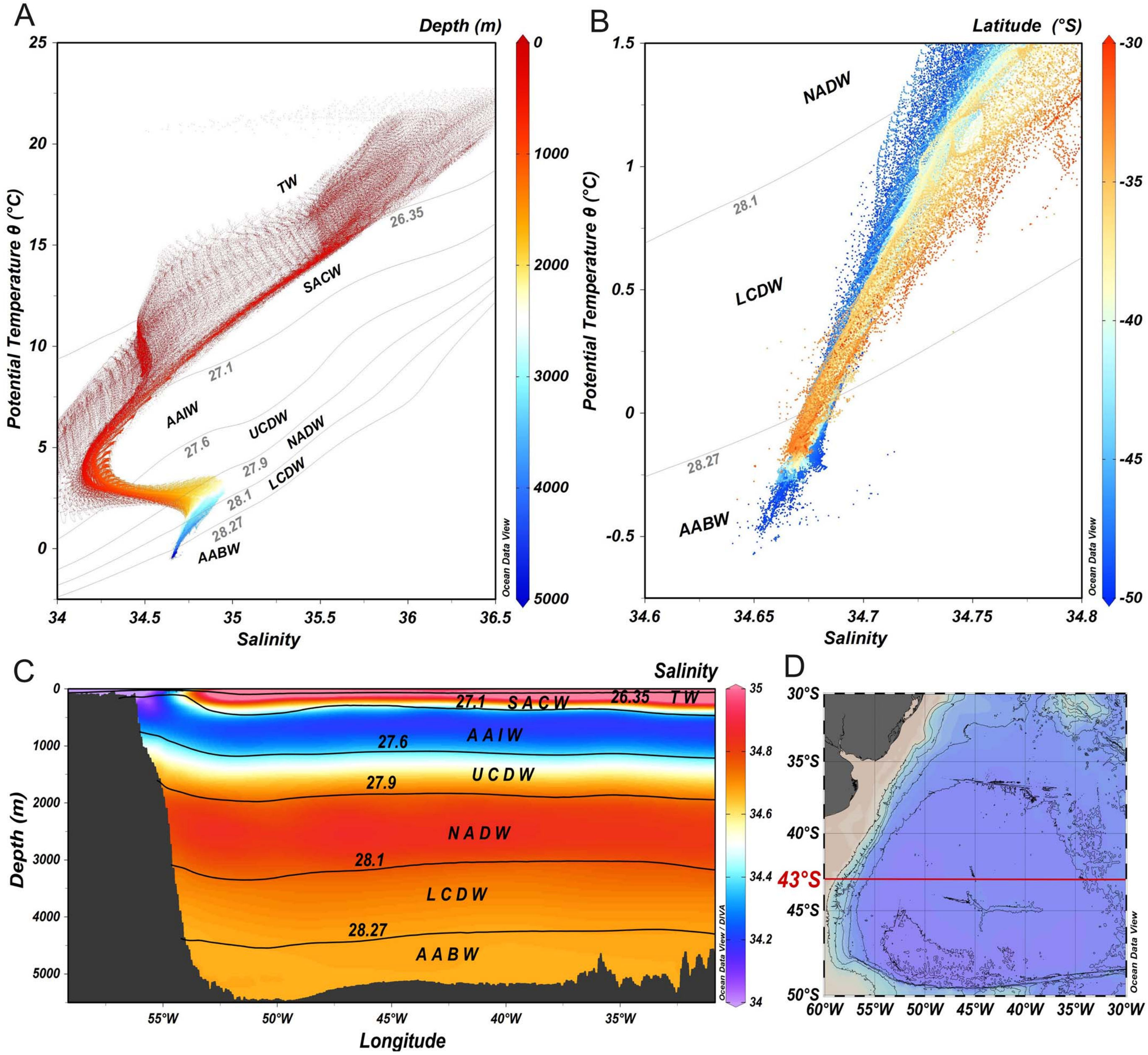

FIG. 2.—Potential Temperature θ (°C). Salinity plots that represent water masses in the Argentine Basin, color bar representing depth in meters **A)** and showing a zoom to the bottom layers with the color bar representing latitudinal location of the water masses. **B)** Solid gray lines indicate neutral density (γ) (kg/m^3) boundaries between different water masses. Hydrographic section at 43° S. **C)** Color bar represents salinity. Isopycnals of neutral density (γn) (kg/m^3) are shown in solid black lines. **D)** Map showing the section from Part C. AABW, Antarctic Bottom Water; LCDW, Lower Circumpolar Deep Water; NADW, North Atlantic Deep Water; UCDW, Upper Circumpolar Deep Water; AAIW, Antarctic Intermediate Water; SACW, South Atlantic Central Water; TW, Tropical Water. Data obtained from World Ocean Atlas 2018 (Locarnini et al. 2018; Zweng et al. 2019), covering the region between 60° W to 30° W in longitude and 30° S to 50° S in latitude.

the long-term cyclonic movement of Antarctic Bottom Water (AABW) and consist primarily of silts and clay (Ewing and Lonardi 1971; Flood and Shor 1988; Hernández-Molina et al. 2008, 2010).

The AB has three major openings that serve as pathways for southern deep and bottom waters (Fig. 1). The westernmost and shallowest is the Malvinas Plateau (Fig. 1), which forms a 2500 m deep saddle between the Malvinas Islands and the and the Maurice Ewing Bank, which peaks at 1200 m (Arhan et al. 1999). The second one is the Malvinas Passage (Fig. 1), a wide break at 35°W 40°W, through which water can enter from the south at a depth of 5000 m (Arhan et al. 1999). The third one is the passage east of the Orcadas Rise (∼ 4500 m depth) (Arhan et al. 1999).

OCEANOGRAPHIC SETTING

Complex patterns of mean flow and variability characterize the ocean circulation in the Argentine Basin (AB). The study area encompasses seven distinct water masses, which exhibit varying characteristics depending on the latitude and depth (Fig. 2). This is due to the convergence of water sources from the Antarctic sector and the North Atlantic in this region (Fig. 1). The Malvinas Passage (Fig. 1) serves as the principal channel for the inflow of Antarctic Bottom Water (AABW) into the AB, encompassing the entire abyssal plain (Fig. 2B, C; Georgi 1981; Solodoch et al. 2021, among others). AABW is formed in several places around Antarctica, such as the Ross Sea, Weddell Sea, Prydz Bay, and Adelie Land (Purkey et al. 2018; Solodoch et al. 2021). Over the AABW is a dense variety of Circumpolar Deep Water (CDW) that circulates around Antarctica within the Antarctic Circumpolar Current, known as the Lower Circumpolar Deep Water (LCDW). The LCDW is the densest water flowing eastward through the Drake Passage. It enters the AB via the Malvinas Plateau (MP), Malvinas Passage (MP), and east of South Georgia, joins the AABW, and flows northward along the western margin of the Argentine Basin (Fig. 1A; Piola et al. 2001; Valla et al. 2018). The Malvinas Current (MC) is a significant component of the flow system in the AB. It is a northern branch of the Antarctic Circumpolar Current (Piola and Gordon 1989). After passing through the Drake Passage, it flows towards the north as a deep-reaching current, with a strong barotropic component and transports sub-Antarctic water. The MC carries cold waters from Antarctic origin, specifically the Subantarctic Surface Water (SASW), Antarctic Intermediate Water (AAIW), and Upper Circumpolar Deep Water (UCDW) (Figs. 1A, 2; Piola et al. 2001). The other distinct flow is the Brazil Current (BC), which has a poleward direction and is the western branch of the South Atlantic subtropical gyre. In contrast to the MC, the BC presents a more baroclinic structure (Da Silveira et al. 2004) and transports warmer and saltier waters that correspond to the Tropical Water (TW) and South Atlantic Central Water (SACW) (Fig. 2; Valla et al. 2018; Piola and Matano 2019). They undergo significant mixing with subantarctic waters at what is known as the Brazil–Malvinas Confluence (BMC) (Fig. 1) region which is widely recognized for its high eddy kinetic energy along with short spatial and temporal scales of velocity fluctuations (Barré et al. 2006; Ferrari et al. 2017; Artana and Provost 2023). This system generates meanders and eddies that promote the thorough mixing of the diverse water masses transported by both currents (Olson et al. 1988; Garzoli and Garraffo 1989; Matano et al. 1993; Provost and Le Traon 1993; Saraceno et al. 2004; Chelton et al. 2007; Paniagua et al. 2018; Orúe-Echevarría et al. 2023, among others). Another relevant water mass reaching the region is the North Atlantic Deep Water (NADW) which flows southward from locations farther north, along the continental margin, and reaching the BMC and then enters the AB (see Valla et al. 2018 for a detailed description of NADW in the South West Atlantic Ocean). The Upper Circumpolar Deep Water (UCDW) is the upper branch of the Circumpolar Deep Water (CDW), a large body of relatively fresh and oxygen-poor water in the Southern Ocean formed by the mixing of upwelling NADW with water circulating in the Antarctic Circumpolar Current (Reid et al. 1977; Valla et al. 2018). The Antarctic Intermediate Water (AAIW) enters the South Atlantic through two distinct routes. The first route is with the MC, which is comparatively colder and fresher (Piola and Gordon 1989), the section at 43° S displays this variety of AAIW (Fig. 2C). The second route is through the Agulhas–Benguela current system, which brings a relatively warmer, saltier, and less oxygenated AAIW (Lutjeharms et al. 1996; Piola and Georgi 1982; Wefer et al. 1996b). In the northern part of the AB, another variety of AAIW can be found. This variety has increased salinity and less oxygen due to recirculation in the subtropical gyre (Valla et al. 2018). The water masses entering the AB from the south are capable of recirculating or flowing northwards and being exported to the Brazil Basin through the Vema Channel (Fig. 1) and the Hunter Channel (Lynn and Reid 1968; Wright 1970; Reid and Nowlin 1971; Buscaglia 1971; Georgi 1982; Speer and Zenk 1993). In the center of the basin lies another characteristic hydrographic pattern of the AB, a strong gyre with barotropic circulation, the Zapiola Gyre (ZG) (e.g., Flood and Shor 1988; Weatherly 1993; Saunders and King 1995; Fu et al. 2001; Fu 2007; Saraceno et al. 2009, among others). The ZG, which has a preferred counterclockwise circulation, revolves around the Zapiola Rise, a geological feature consisting of sedimentary deposits on the ocean floor (Saunders and King 1995; de Miranda et al. 1999). In the Zapiola Rise region, the ocean floor's topography plays a crucial role in determining the trajectory of eddies (Saraceno and Provost 2012). The wide range of spatial and temporal scales involved in these dynamic processes makes the AB a highly interesting location for studying the interplay of oceanic variability across different scales (Fu 2007).

METHODS AND DATA

GLORYS12 Velocity Data

To compute the bottom velocities, we used the GLORYS12 reanalysis. GLORYS12 is a global eddy-resolving physical ocean and sea-ice reanalysis at 1/12° horizontal resolution covering the 1993–present altimetry period, designed and implemented in the framework of the Copernicus Marine Environment Monitoring Service (CMEMS) (http://marine.copernicus.eu/). Ocean reanalysis aims at providing the most accurate past state of the ocean in its four dimensions (Lellouche et al. 2018). GLORYS12 is based on the current real-time global forecasting CMEMS system PSY4V3 (Lellouche et al. 2018). The vertical grid has 50 levels with 22 levels in the upper 100 m, leading to a vertical resolution of 1 m in the upper levels and 450 m resolution for the deepest levels up to a maximum depth of 5727 m. The reanalysis is performed with a numerical model whose physical component is the Nucleus for European Modeling of the Ocean (NEMO) (Madec et al. 2008). The model assimilates observations using a reduced-order Kalman filter with a 3-D multivariate modal decomposition of the background error and a seven-day assimilation cycle (Lellouche et al. 2013). Along-track satellite altimetric data from CMEMS (Pujol et al. 2016), satellite sea-surface temperature from NOAA, sea-ice concentration, and *in situ* temperature and salinity vertical profiles from the latest CORA *in situ* databases (Cabanes et al. 2012; Szekely et al. 2019) are jointly assimilated. A 3-D-VAR scheme provides an additional 3-D correction for the slowly evolving large-scale biases in temperature and salinity when enough observations are available (Lellouche et al. 2018). GLORYS12 reanalysis has been shown to correctly reproduce hydrography and velocities in the Argentine Basin and the Drake Passage, as compared with current-meter data in the water column and near the seafloor (Artana et al. 2018a, 2018b, 2021a, 2021b; Poli et al. 2024).

To cover the deepest locations in the AB, we extracted 20 depth levels corresponding to the depths from 453 m to 5727 m. With a focus on the period since satellite altimetry measurements of sea level have provided reliable information on ocean eddies, a daily data set is used that spans from 1 January 1993 to 31 December 2020 (28 years eq. to 10,227 days). The chosen variables are the Eastward Sea water velocity *uo* (m/s) and the Northward Sea water velocity *vo* (m/s). The longitude was considered from 60° W to 30° W (362 values), the latitude from 30° S to 50° S (241 values). With this data, we have built a four-dimensional data cube of longitude, latitude, depth, and time (362, 241, 20, 10,227). The procedure consists in computing all 20 levels together to extract the value at each time and from the model cell closest to the bottom. We computed the mean speed and the mean direction of the bottom-current velocity in m/s and the bottom eddy kinetic energy (EKE) in m^2/s^2. The EKE is defined as the energy contained in the time-varying component of ocean velocities, which are measured as anomalies in velocity. To calculate the EKE, we first compute the anomalies for the *v* and *u* components, and then use Equation 1.

$$EKE = {}^{1}\!/_{2}\,(u'^{2} + v'^{2}) \tag{1}$$

u' and *v'* denotes velocity anomalies.

Hydrographic Data

To determine the water masses in the Argentine Basin, The World Ocean Atlas 2018 (WOA18) was used (Locarnini et al. 2018; Zweng et al. 2019). WOA18 is a collection of objectively analyzed, quality-controlled temperature, salinity, oxygen, phosphate, silicate, and nitrate means based on profile data from the World Ocean Database (WOD).

Geophysical Data and Grain-Size Measurements

The large-scale distribution of contourite features used in this study is mainly based on the original maps provided by Ewing and Lonardi (1971), Flood and Shor (1988), and Hernández-Molina et al. (2010) (Fig. 1A); only the crest of the Zapiola drift has been updated using the bathymetry of the GEBCO 2023 Grid, which has a 15-arc-second interval grid (GEBCO Compilation Group 2023).

Sub-bottom profile images shown in the present study were collected with the hull-mounted, parametric PARASOUND sediment echosounder system during the RV Meteor cruises M29/1 and M46/3 in 1994 (Segl 1994) and in 2000 (Bleil 2001). The parametric frequency was set during both cruises to 4 kHz, providing a penetration down to 100 m and a vertical resolution at decimeter scale. To improve the signal-to-noise ratio, the data were filtered with a wide bandpass filter of 2.5–5.5 kHz. A trace envelope was calculated to enhance reflector coherency. PARASOUND profiles were analyzed and visualized using "The Kingdom Software" (IHS Markit). PARASOUND profiles were used in this study to identify and characterize recent contouritic features (contourite drifts, sediment waves, channels, and erosional surfaces, among others).

Multi-channel seismic reflection profile BGR98-40 was collected by the Federal Institute for Geosciences and Natural Resources (BGR) in 1998, using an air gun on the vessel Akademik Lazarev. This profile was used to identify contourite features in an area where PARASOUND data are absent or of insufficient quality. The nomenclature and criteria to identify contourite features is based on Faugères et al. (1999), Faugères and Stow (2008), Nielsen et al. (2008), Rebesco et al. (2014), and Miramontes et al. (2021).

In this study, we use the sand content of surface sediments (0–1 cm or 0–2 cm below the seafloor) obtained from Frenz et al. (2004) and Petschick et al. (1996) by sieving, which are publicly available in the PANGAEA repository (Frenz et al. 2004; Petschick et al. 1996). Additional surface sediments (0–1 cm or 1–2 cm below the seafloor) from R/V Meteor cruises M23/2, M29/2, M46/3, and M49/2 (Bleil 1993, 1994, 2001; Spieß 2002) were measured for this study using the laser-diffraction particle size analyzer LS13320 (Beckman Coulter) in MARUM laboratories, which measured particle grain size from 0.04 to 2000 μm (Miramontes et al. 2024). In this study, only sand percentages (the 63–2000 μm fraction) are shown in order to be able to compare with the data from previous studies which were obtained by sieving. The samples were collected with different devices: gravity corer, multi corer, or giant box corer. The type of device used for sampling for each core is detailed in the documents available in PANGAEA (Frenz et al. 2004; Petschick et al. 1996; Miramontes et al. 2024).

RESULTS

Mean Circulation in the Argentine Basin

The surface mean velocities at the Argentine Basin (AB) (Fig. 3A), calculated with GLORYS12 reanalysis daily data spanning 28 years (1 January 1993 to 31 December 2020), align well with altimetric data previously published (e.g., Ferrari et al. 2017; Artana et al. 2019, 2021b; Artana and Provost 2023). The average surface velocity clearly displays the jets originating from the Malvinas Current (MC) between the North Boundary (NB) and the Sub Antarctic Front (SAF). The Brazil Current (BC) and the overshoot (e.g., Saraceno and Provost 2012; Ferrari et al. 2017) have been well resolved as the Malvinas return flow (Fig. 3A). Low mean speeds are observed in the central area of the Zapiola Gyre location, which is consistent with the findings of Saraceno et al. (2009) and Artana and Provost (2023) (Fig. 3A). Figure 3B illustrates the maximum recorded surface speed on 5 March 2008, at longitude 48° 34′ W and latitude 40° 9′ S, measuring 3.5 m/s. Intense mesoscale eddies are well resolved with the GLORYS12 reanalysis (Fig. 3B) linked to the interaction and dynamics of the BMC, the Polar Front (PF), the Sub Antarctic Front (SAF) and the North Boundary (NB) fronts from the Antarctic Circumpolar Current (ACC) in the AB.

The mean bottom-velocity field, illustrated in Figure 3C, depicts the movement of deep water entering the basin from the south. One of the paths runs through the Malvinas Passage, which turns westward and follows the Malvinas Escarpment (Fig. 3C). In this flow, the highest average value for all AB was found to be 0.52 m/s. The second route of deep waters is positioned in the SAF and flows northward towards the confluence zone. This flow represents an offshore component of the MC and occurs between depths of 1000 m in some areas and greater than 2000 m in others. This observation aligns with the findings of Frey et al. (2023). The ZG (e.g., Saraceno et al. 2009) is resolved in the mean bottom current, as shown in Figure 3C. The gyre exhibits an anticyclonic rotation in the mean field. The Zapiola Rise is present within the gyre's domains, and the distinct flow pattern is caused by topographical features as Saraceno et al. (2009) show. The most energetic regions (Fig. 3D) align with high surface mesoscale zones in the BMC, where the flow passes through the Malvinas Passage as described above. The low variability of the SAF flow is indicated by the low EKE values. Additionally, in the northeastern region of the AB and over the ZD, low EKE values are observed at the bottom, in agreement with Artana and Provost (2023) that they show the same feature for the surface using satellite altimetry.

Contourite Features and Related Bottom Currents

The central deep part of the basin is dominated by a large contourite drift, the Zapiola Drift (ZD) (Fig. 1A), which has a relief of over 1000 m in some areas, especially in the southern part. The drift has a main crest, which is around 1000 km long and has a W–E orientation. The primary ridge is situated in water depths ranging from 5400 m in the west to 4700 m in the east (Fig. 1A). Secondary crests, which are 150–350 km long, are oriented almost perpendicular or oblique to the main crest, with N–S, NNE–SSE orientation (Fig. 1A). The secondary crests are located at water depths that range between 5000 m in the northern part and 5500 m in the southern part. The ZD is composed of fine-grained sediments, with sand contents below 12% (Fig. 4A). The grain-size measurements are consistent with PARASOUND profiles, which show relatively high penetration of the signal and continuous reflections, which is typical of muddy sediments (Fig. 4C). Large areas of the ZD are covered by sediment waves (Fig. 4C; Flood and Shor 1988; von Lom-Keil et al. 2002). The height of the sediment waves tends to decrease towards the western edge of the drift, and sediment waves are absent in the lower part of the drift (Fig. 4C). At the foot of the western part of the drift, the seafloor is clearly dominated by erosion and winnowing, with abundant truncated reflectors at the seafloor and low signal penetration in the PARASOUND data, which is typical of relatively coarse-grained sediments (Fig. 4C), as confirmed by grain-size measurements that show sand contents of up to 39% (Fig. 4A).

In this area, mean bottom currents show maximum values of 0.27 m/s in the western part of the drift crest. There seems to be no clear correlation between mean current velocity and the observed distribution of the contourite features and grain-size observations (Fig. 4A). For example, the area of the drift crest characterized by the presence of fine sediments corresponds to a zone with relatively high mean modeled bottom currents, while the modeled bottom currents are weaker in the zone dominated by winnowing and erosion (Fig. 4A, C). In contrast, bottom EKE of this region exhibits a distribution similar to contourite features and grain size. The main zone of accumulation of the ZD, composed of muddy sediments, is located in an area of low bottom EKE. In contrast, the zone characterized by coarser sediments and erosional surfaces is under the influence of high bottom EKE (Fig. 4B).

The continental slope of the Argentinean margin is composed of a series of contourite terraces, which are relatively flat surfaces, commonly composed of sandy sediments and with common erosional features (Figs. 1A, 5A; Hernández-Molina et al. 2010; Gruetzner et al. 2011; Wilckens et al. 2021). A separated mounded drift and a moat is found at the foot of the slope, along the Malvinas Plateau, with a sand content of 28% (Fig. 5A). Surface sediments at the Perito Moreno Terrace, located at 1000–2000 m water depth, are almost purely composed of sand (about 98%) and the terrace shows common erosional surfaces (Fig. 5A, C). Strong mean bottom currents (0.2–0.3 m/s) related to the MC affect the Perito Moreno Terrace (Fig. 5A, B). Bottom-current speed is much weaker between 2000 and 5000 m

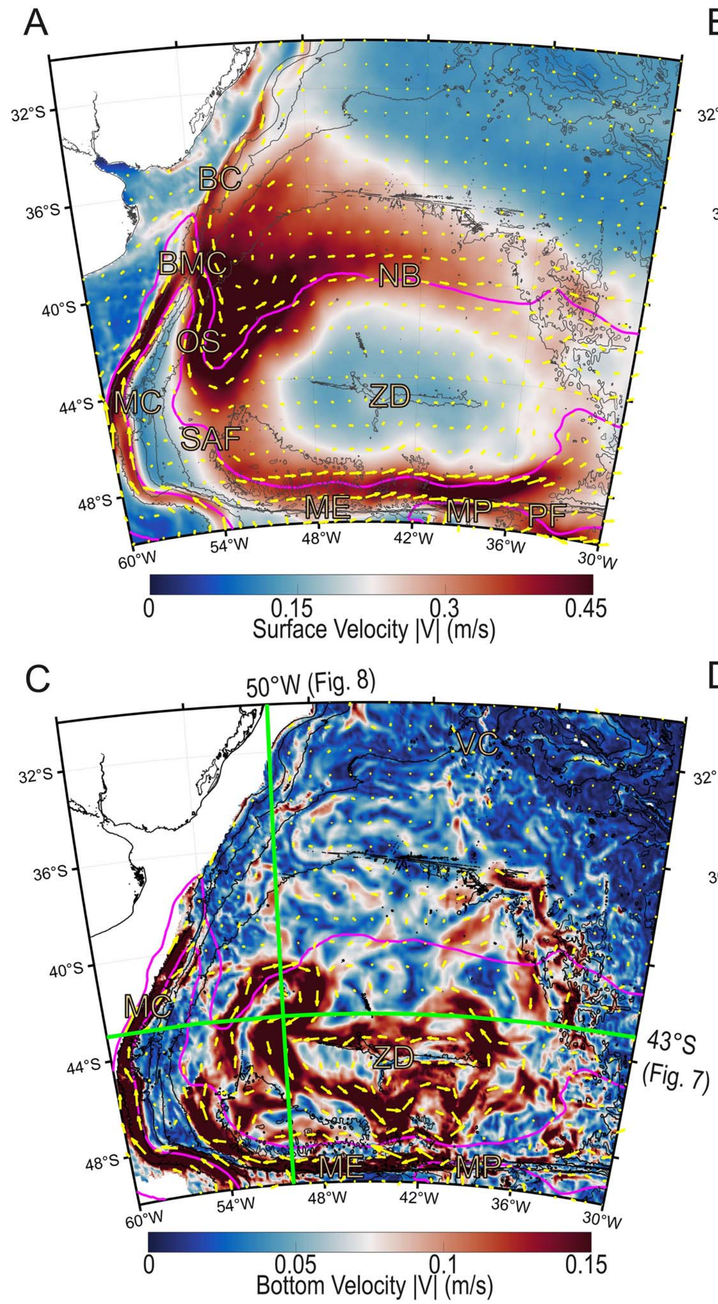

FIG. 3.—**A)** Mean velocity (m/s) at sea surface in the Argentine Basin, calculated during 1993–2020 from GLORYS12 reanalysis. **B)** Sea-surface velocity (m/s) at the day with highest speed (3.5 m/s), on 5 March 2008, at longitude 48° 34′ W and latitude 40° 9′ S. **C)** Mean velocity (m/s) at bottom layer in the Argentine Basin, calculated during 1993–2020 from GLORYS12 reanalysis. **D)** Bottom eddy kinetic energy (EKE) (m^2/s^2) 1993–2020. Depth contours are shown every 1,000 m with black lines. The mean locations of the Antarctic Circumpolar Current fronts derived from satellite altimetry (Park et al. 2019) and Park and Durand (2019) are indicated with solid pink lines, NB, North Boundary; SAF, Sub Antarctic Front; PF, Polar Front; MC, Malvinas Current; BC, Brazil Current; BMC, Brazil–Malvinas Confluence; OS, Overshoot; ZD, Zapiola Drift; ME, Malvinas Escarpment; MP, Malvinas Passage; VHC, Vema Channel; AP, abyssal plain; ZG, Zapiola Gyre. The yellow arrows indicate the directions and intensities of mean currents. Green lines represent location of the section to extract time series.

water depth, with mean speeds below 0.1 m/s and often even below 0.05 m/s, in agreement with the presence of finer surface sediments (Fig. 5A, D). Another zone of intense bottom currents, with mean speeds of 0.2–0.3 m/s, is found at 5000–6000 m water depth. These strong bottom currents are consistent with the presence of contourite channels in this area (Fig. 1A; Hernández-Molina et al. 2010).

The alternation of sandy contourite terraces and muddy contourite drifts is not exclusive to the southern part of the margin; it is also present in the northern area (Fig. 6). In this zone, bottom currents related to the MC oscillate between 0.2 and 0.35 m/s and control the deposition of sandy sediments with sand contents of 94–99%. Below 2000 m water depth, mean bottom current speed decreases, with values below 0.1 m/s, and the content of sand also generally decreases, typically ranging between 30 and 52% (Fig. 6A). A moat and a separated mounded drift are located at the foot of the slope. The moat is located in a zone where mean bottom currents are slightly higher (0.1–0.15 m/s) and the contourite drift is

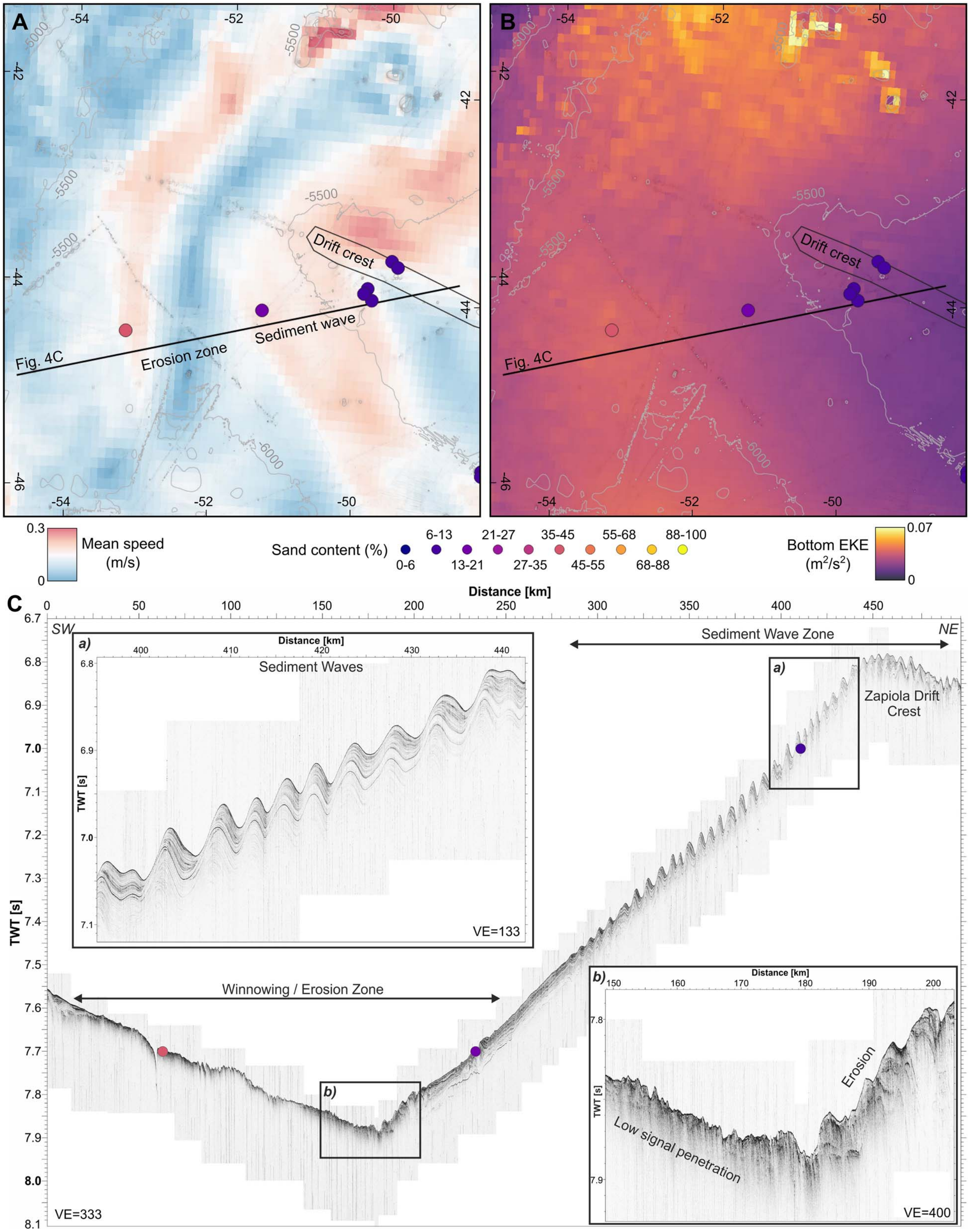

FIG. 4.—**A)** Mean bottom-current speed (m/s) from GLORYS12 reanalysis and sand content of surface sediments. See Figure 1 for location. **B)** Bottom eddy kinetic energy (m^2/s^2) from GLORYS12 reanalysis and sand content of surface sediments. The position of the crest of the Zapiola Drift is indicated with a black line. **C)** PARASOUND sub-bottom profile GeoB00-036PS showing the transition from an area on the west dominated by winnowing and erosion to the Zapiola drift on the eastern side, which is dominated by fine-grained sediments and covered with sediment waves. Colored circles indicate sand content of surface sediments and are projected on the profile from core locations located slightly north of the profile (see Part 4A).

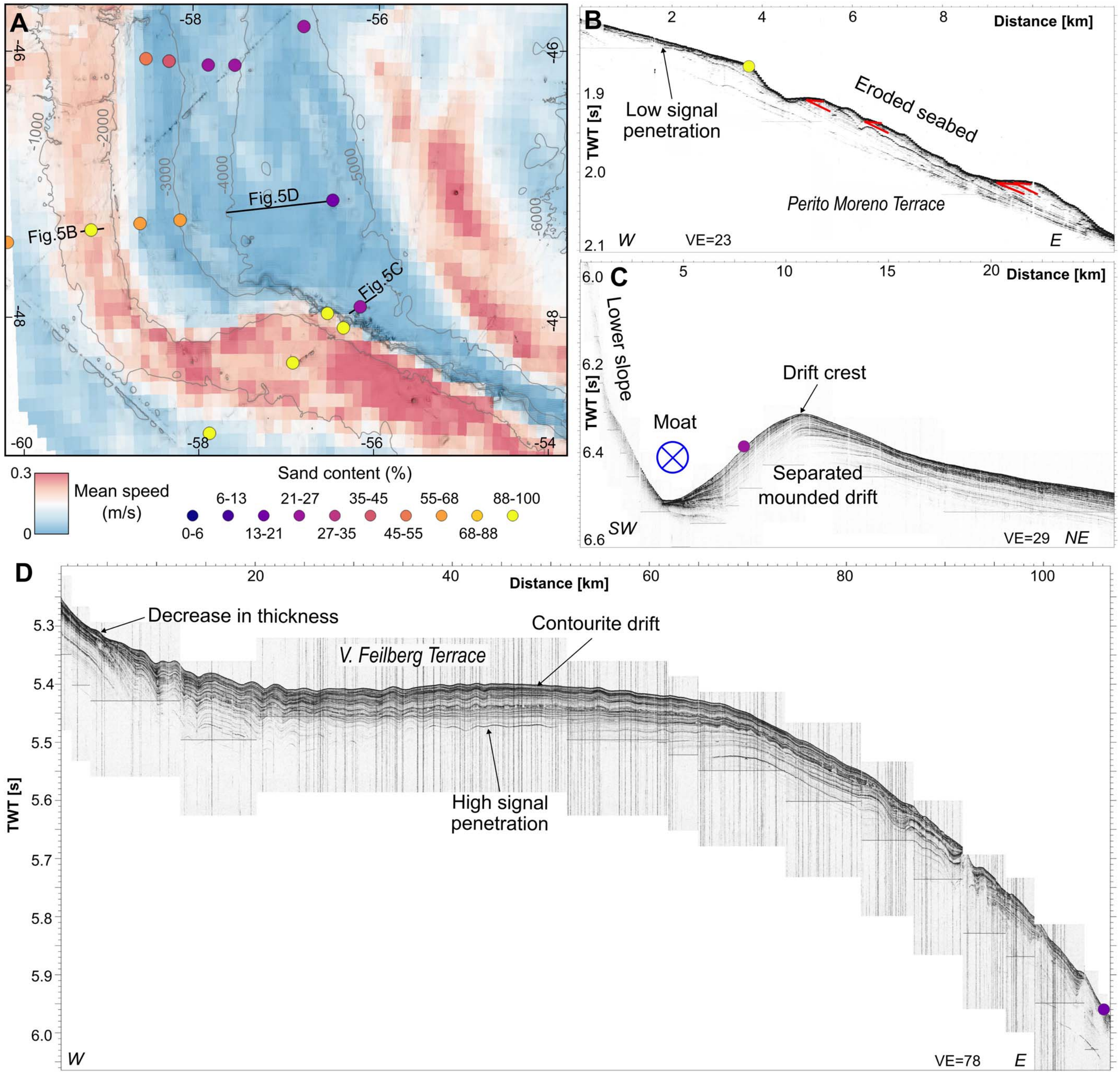

FIG. 5.—**A)** Mean bottom-current speed (m/s) from GLORYS12 reanalysis and sand content of surface sediments. See Figure 1 for location. **B–D)** PARASOUND sub-bottom profiles showing different depositional and erosional contouritic features found on the SW part of the Argentinean continental margin, and sand content of surface sediments. Red arrows in Part B highlight erosional truncations.

located in the adjacent zone of weak bottom currents, with mean speeds below 0.05 m/s (Fig. 6).

Variability of Bottom Currents

The time series of bottom currents, or Hovmöller diagrams, at a fixed latitude and longitude (see Figure 3C for the location of the sections) are shown in Figures 7 and 8. These data provide valuable insight into changes in bottom currents. Figure 7 shows the time series at a fixed latitude of 43° S, covering the AB from west to east over the entire time period (01-01-1993 to 31-12-2020). At the west bottom currents are dominated by the entrance of the MC, which flows in a south-to-north direction. The MC flows across water depths ranging, in our case, from 453 to the ocean floor (~ 2500 m) (see Fig. 3C), in agreement with Vivier and Provost (1999) and Piola et al. (2001). The MC is considered an equivalent barotropic current and with multiple jets (Matano et al. 1993; Peterson and Whitworth 1989; Peterson et al. 1996; Piola et al. 2013); here we detect the offshore branch (Piola et al. 2013; Frey et al 2023). Since the GLORYS12 reanalysis is categorized as a barotropic model, and the baroclinic component is not as well depicted (Artana et al. 2021a, 2021b), the MC offshore branch is well illustrated at the bottom (Fig. 3C). On closer examination, it is evident that there have been periods of weakness in the MC, which is consistent with the findings of

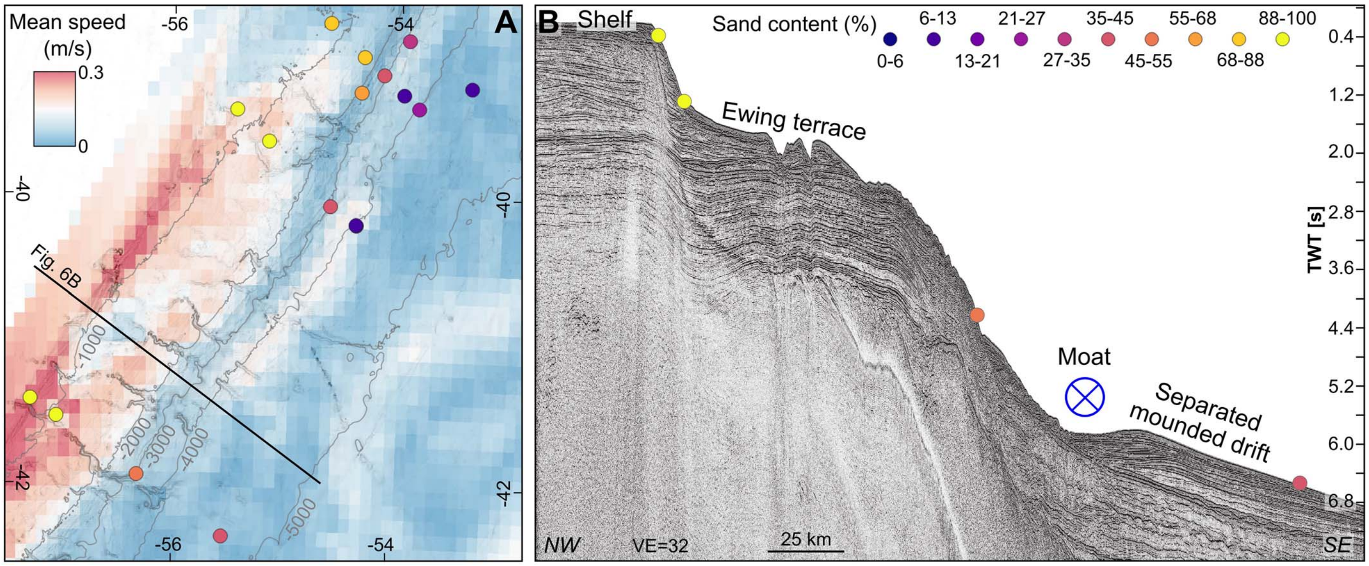

FIG. 6.—**A)** Mean bottom-current speed (m/s) from GLORYS12 reanalysis and sand content of surface sediments. See Figure 1 for location. **B)** Seismic profile BGR98-40 showing the Ewing terrace on the slope and a moat-drift system at the foot of the slope, as well as sand content of surface sediments projected on the profile (real measurements done farther south, see Part A). Part B is modified from Gruetzner et al. (2011).

Ferrari et al. (2017), Artana et al. (2018a, 2018b) Paniagua et al. (2018), Orué-Echeverria et al. (2019), among others (Fig. 7). It is worth noting that the reanalysis (Fig. 7) resolves sporadic migration of the MC to the east at 43° S (e.g., 1996, 2005, 2010, 2015, 2018, 2019, and 2020). East of the MC, bottom currents at the slope present low intensity (Fig. 7). Between 55° W and 48° W, the bottom of the BC shows a discernible overshoot, with two distinct patterns, one with a northward flow and the other with a southward flow (Fig. 3C). This region of high EKE (Fig. 3D) can be distinguished in the time series by the intermittent intensity of the bottom currents (Fig. 7). Moving eastward at 43° S, we found a region north of the main ZD crest

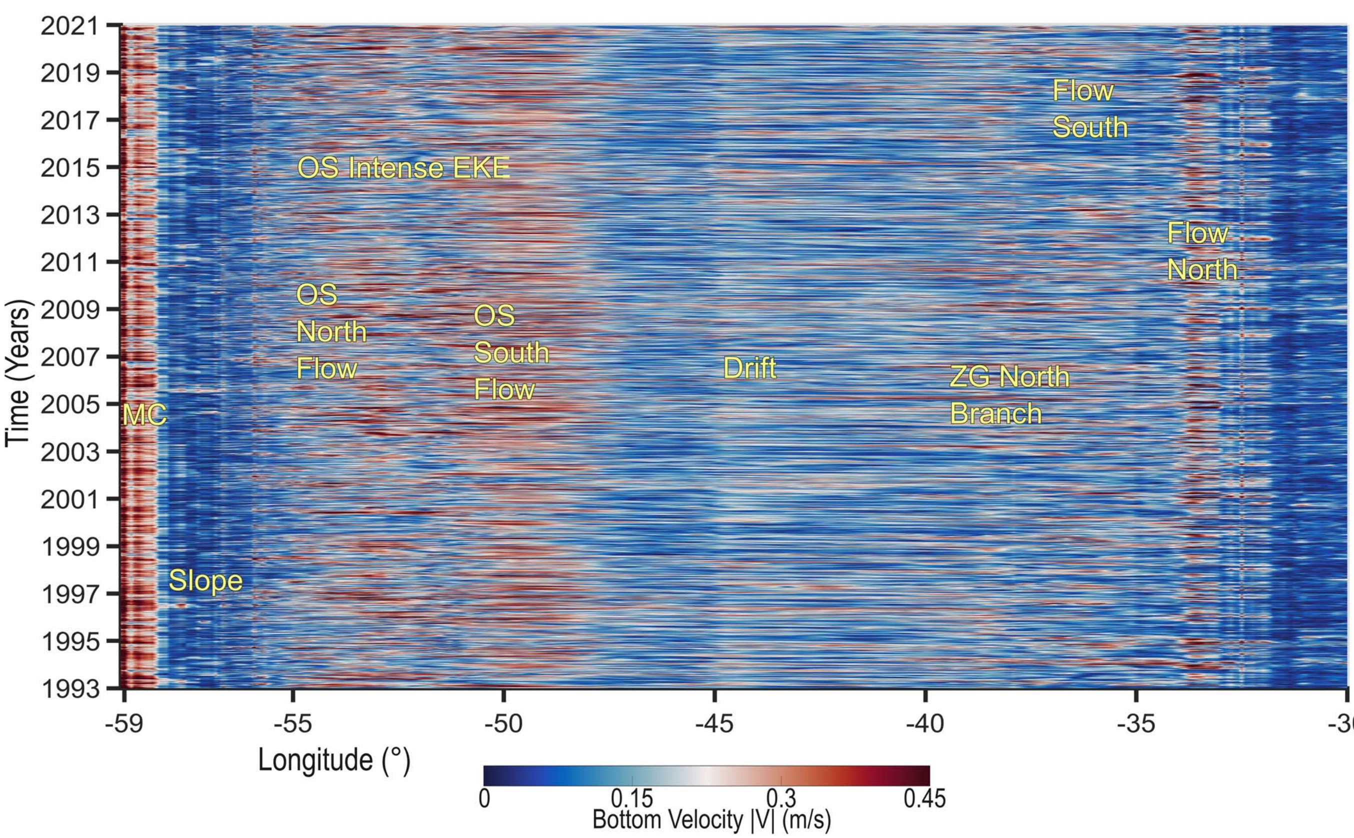

FIG. 7.—Time series (1 January 1993 to 31 December 2020, 28 years) of mean bottom velocity (m/s) along track at latitude 43° S (see location in Fig. 3C). Position of main flows are represented. MC, Malvinas Current; OS, Overshoot; ZG, Zapiola Gyre; EKE, eddy kinetic energy.

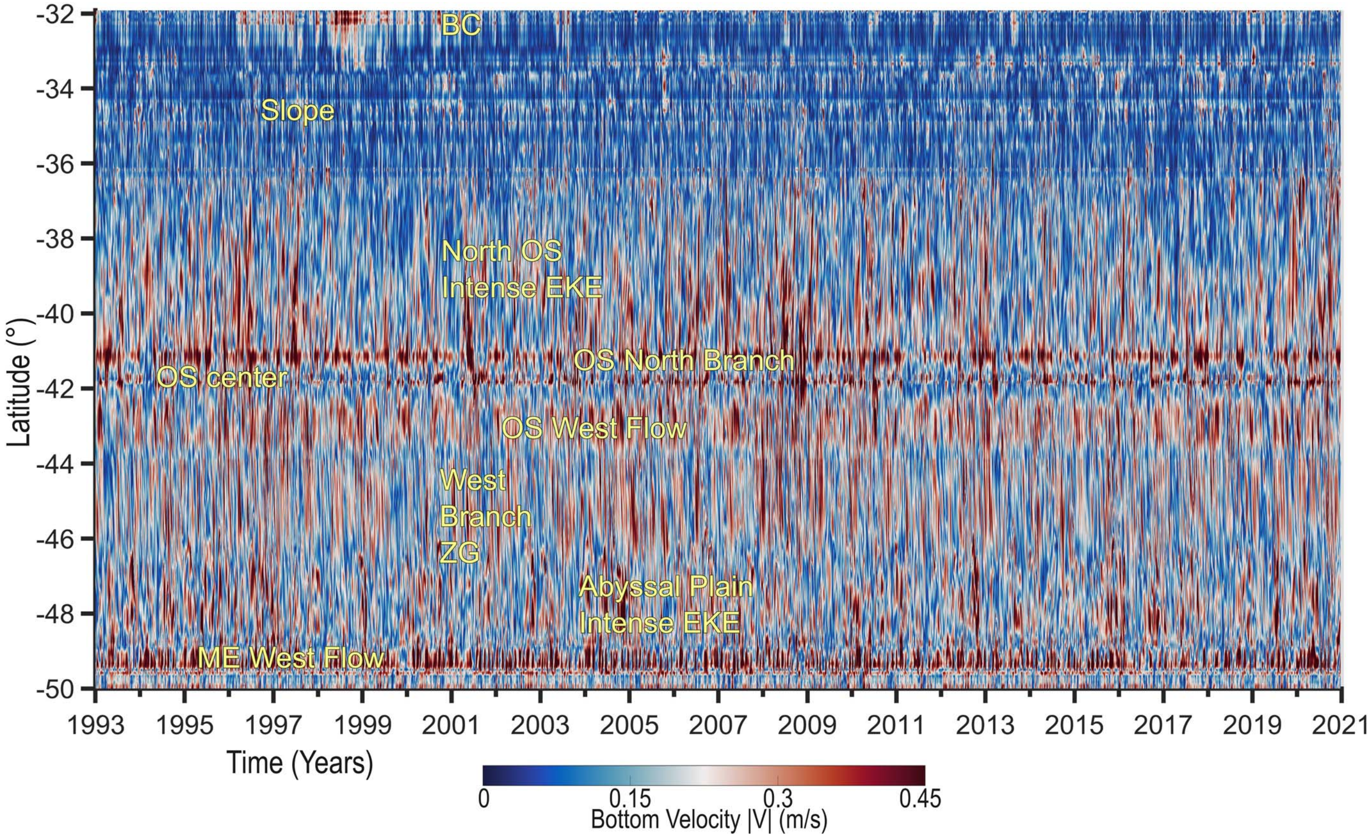

FIG. 8.—Time series (1 January 1993 to 31 December 2020, 28 years) of mean bottom velocity (m/s) along track at longitude 50° W (see location in Fig. 3C). Position of main flows are represented. ME, Malvinas Escarpment; OS, Overshoot; ZG, Zapiola Gyre; EKE, eddy kinetic energy; BC, Brazil Current.

with the presence of a small drift crest (Fig. 1A), which shows relatively slow currents (Figs. 3C, 7). The events with strong currents could be associated with movements of the northern branch of the ZG to the north (Figs. 3C, 7). Around 38° W, the north branch of the ZG can be distinguished in the time series (Fig. 7); this pattern presents intermittently strong and weak events. The southward flow near 36° W (Fig. 7) appears to be part of a small cyclonic circulation originating from the north branch of the ZG (Fig. 3C). This flow follows the bathymetric contour of 5000 m. When it reaches 44° S, it turns east and enters a region of complex topography and flows north as shown in Figure 7. This northerly flow has an intense activity during the analysis period (Fig. 7). It appears that this flow later feeds the Vema Channel (Fig. 3C).

The Hovmöller diagram calculated for a fixed longitude of 50° W shows distinct patterns in bottom currents from south to north (Fig. 8). The westward flow over the ME is consistently strong around 49° S (Fig. 8). The intense EKE activity in the abyssal plain (Fig. 3D) is shown in the time series with intermittent fluctuations of the bottom current (Fig. 8). In the band between 44° S and 46° S the western branch of the ZG (Fig. 3C) is observed, and periods of low activity (e.g., year 2000) or intense activity (e.g., year 2008) are clearly visible in the time series (Fig. 8). The overshoot later turns to the west, and this current subsequently joins the west branch of the ZG (Fig. 3C). The transect at 50° W crosses a low-velocity field in the mean bottom current (Fig. 3C) as in the center of the overshoot. In the time series (Fig. 8) we observe that this center represents strong events as low ones, suggesting the movement and strong EKE of this region. The northern branch of the overshoot is stronger over time and presents fewer slow periods (Fig. 8). North of this northern branch a band of intense EKE is also revealed with intermittent events in the bottom currents (Fig. 8). Between 1996 and 2001, a significant event with a peak in 1998 was detected at 32° S (Fig. 8). The strong variability of the BC (Mata et al. 2012) and the trend of BC to be nearer to the 800-meter isobath (Schmid and Majumder 2018) could be related to this finding.

DISCUSSION

Hernández-Molina et al. (2009, 2010) and Preu et al. (2013) propose that the powerful boundary currents in the Argentine Basin have significantly altered and redistributed bottom sediments, resulting in the creation of a substantial contourite depositional system including large terraces over extended geological time periods. The GLORYS12 reanalysis revealed that the bottom velocities speed up to 1.05 m/s in the area where the Malvinas Current (MC) flows. Furthermore, the barotropic current is depicted, exhibiting a pronounced flow in the offshore branch (Fig 3C). For example, Piola et al. (2013), Paniagua et al. (2018), and Frey et al. (2023) corroborate this feature with *in situ* observations at different locations in the MC path. The powerful MC in the lower layer affects sediment patterns differently than in the Zapiola Drift (ZD) area. The current in the MC path is predominantly consistent (Fig. 7), yet exhibits low levels of EKE (from ~ 0.003 m^2/s^2 to ~ 0.01 m^2/s^2) (Fig. 3D). Moats (EKE ~ 0.015 m^2/s^2, Fig. 5C, ~ 0.009 m^2/s^2, Fig. 6B) are present in zones of higher velocity and separated drifts (EKE ~ 0.008 m^2/s^2, Fig. 5C, ~ 0.009 m^2/s^2, Fig. 6B) in surrounding regions of lower speeds. In other regions exhibiting contourites, such as the Mozambique channel, EKE levels are relatively low. For instance, in abraded surfaces and moats, the EKE value is approximately 0.005 m^2/s^2, while for terraces it is 0.003 m^2/s^2 (Miramontes et al. 2021). Wilckens et al. (2021) demonstrated that the (paleo) MC caused erosion on the slope, which in turn cut the slope landward and widened the contourite terrace over time. Such events at the bottom layer may alter sediments in ways beyond solely considering the mean value of the current.

In this study, we observe that bottom currents are strongly influenced by the main margin morphology. Areas of strong currents are characterized by terraces, while areas of weak currents exhibit contourite drifts (Fig. 5), a pattern that is analogous to the observations made in the Mediterranean Sea (Miramontes et al. 2019a). The deep Malvinas Current exhibits a relatively homogeneous bottom-current pattern along the entire Perito Moreno Terrace, which displays pronounced erosional surfaces, particularly in its central region (Fig. 5A, B). In contrast, in the northern part of the Ewing Terrace, strong bottom currents are focused on the landward part of the terrace, where an abraded surface and a moat are found (Fig. 6; Wilckens et al. 2021). However, in both instances, the sedimentation process intensifies in the vicinity of low current velocities, leading to the formation of a contourite drift (Figs. 5C, 6B; Wilckens et al. 2021). This suggests that probably alongslope bottom currents are one of the main factors controlling contourite-terrace formation. It has also been suggested that contourite terraces may be related to internal waves propagating at the interface of water masses (Hernández-Molina et al. 2016; Thiéblemont et al. 2019). But, it is unclear whether internal waves alone can entirely form contourite terraces or if they are only a secondary process that can reshape terraces and form, for example, channels or dunes on top of contourite terraces (Miramontes et al. 2020, 2021).

The formation of contourite depositional systems is commonly attributed to relatively constant or persistent bottom currents (Rebesco et al. 2014, and references therein). Nevertheless, an increasing number of studies indicate that bottom currents exhibit considerable spatial and temporal variability. These changing conditions are likely to play a significant role in the formation of contourites (Thran et al. 2018; Miramontes et al. 2019a, 2019b, 2021; Kreps et al. 2023; Zhao et al. 2024). Ocean currents in the Argentine Basin are known to present episodes of very intense velocity, especially related to eddies with observed peaks of 0.9 m/s in the upper 500 m of the water column (Artana and Provost 2023). In our study, we show that these extreme events are also present in the bottom, with velocities that can reach up to 1.23 m/s in the region of the overshoot (Figs. 4, 8). As noted by Ferrari and Wunsch (2009), the variations experienced by the currents are closely related to mesoscale activity and dominate the oceanic kinetic-energy reservoir. The intensity of this activity varies from region to region, and the bottom EKE in the Argentine Basin is among the largest in the world (Thran et al. 2018). The regions in the Overshoot and abyssal plain are the ones with higher EKE activity up to 0.09 m^2/s^2 (Fig. 3D). It is notable that the region near the Zapiola Drift, where the surface velocity field is relatively low (Fig. 3A), and also the EKE is low (e.g., Saraceno and Provost 2012; Artana and Provost 2023), the bottom layer displays more activity in the bottom currents near topographic changes (Fig. 3C). The relatively low EKE ($\sim$ 0.01 m^2/s^2) around the ZD indicates a more persistent flow (Fig. 3C, D), which is associated with the presence of the Zapiola Gyre (ZG). As one moves away from the ZG, the EKE increases ($\sim$ 0.03 m^2/s^2) (Fig. 3D). Poli et al. (2024) recently found that this situation corresponds to stable ZG with high values in transport. However, events where there is an inverse in this situation are related to collapses of the ZG; this situation is more permeable to mesoscale activity around the ZD (Poli et al. 2024).

In the western region of the ZD, erosion and winnowing have resulted in relatively coarse-grained sediments (Fig. 4C). The time series provide evidence of strong bottom currents that influence sedimentation patterns in this region (Fig. 8). It is evident from Figure 3C that the southern branch of the overshoot contributes to the western branch of the ZG. Flood and Shor (1988) suggest that a strong anticyclonic circulation has existed near the ocean floor for thousands of years, as indicated by the orientation of the mud waves present around the Zapiola Rise. We observed a gradual decrease in the height of sediment waves towards the western edge of the drift, which may be caused by lower sedimentation rates due to stronger and more variable currents (Fig 4C; von Lom-Keil et al. 2002). Furthermore, sedimentary waves did not occur in the lower section of the drift, as shown in Figure 4C. The sediment waves are mainly oriented perpendicularly or oblique to the main crest of the ZD, as observed in other drifts of the Antarctic Peninsula (Rodrigues et al. 2022), in agreement with a main flow following the contours of the drift. It is however still unclear what processes exactly control the development and evolution of sediment waves. It has been suggested that the passage of eddies can result in the formation of irregularly oriented sediment waves (Breitzke et al. 2017; Fierens et al. 2019), and that sediment waves can be formed by propagation of internal waves at the benthic thermocline cap (Kolla et al. 1980) or by the formation of lee waves or flow-field perturbations related to wavy or irregular topography (Flood 1988; Hopfauf and Spieß 2002).

CONCLUSION

The present interdisciplinary study investigated the circulation of bottom current and their impact on sedimentation in the Argentine Basin. The bottom-currents circulation was analyzed using GLORYS12 reanalysis data obtained over 28 years. Sediment analysis relies on hydrographic, bathymetric, hydroacoustic, seismic data, and sediment cores.

Contouritic sedimentation in certain areas may primarily be influenced by mesoscale activity, such as ocean eddies and meandering currents. This activity undergoes intermittent processes over time alternating between strong and weak events in the current flow, while in other areas, sedimentation is regulated by constant flows where mesoscale activity is minimal. In the center of the AB, the Zapiola Drift is encircled by a region exhibiting high bottom eddy kinetic energy that led to the erosion of the seafloor and sedimentary buildup consisting of sandy mud. The highest EKE surrounding the ZD at the seabed is located in the region of the overshoot of the Brazil Current and in the deepest part of the abyssal plain. On the west part of the AB, the Malvinas Current flows strongly and persistently northwards along the continental slope and exhibits minimal EKE at the bottom compared to the extremely high regions of EKE mentioned above. Despite the relatively low EKE, the MC at the bottom is constrained by the topography and has a sporadic migration in space and time to the east, i.e., basinward to the deepest locations.

The region of the continental slope through which the MC travels is marked by a contourite terrace, a comparably even subsurface consisting mainly of sandy sediments with numerous erosional traits. We suggest that relatively constant along-slope bottom currents, such as the MC, play a major role in the formation of contourite terraces. In contrast, sedimentation in the abyssal plain seems to be dominated by extreme events of high intensity related to eddies of the overshoot of the BC that induce erosion in the western part of the Zapiola Drift.

The time series of bottom currents depicts the variability and intermittent activity and illustrates how the mesoscale activity and constant flows dominate the AB. Combined with the analysis of the EKE and the mean current field at the bottom, it provides an insight into bottom-current dynamics. Further studies should consider evaluating the connectivity between regions in relation to propagation of bottom currents. Additionally, the lack of *in situ* data should prompt the continuation of research campaigns to evaluate this critical area in the global climate, specifically as a point in the Atlantic Meridional Overturning Circulation.

ACKNOWLEDGMENTS

We thank captain and crew as well as all Parasound watchkeepers of RV *Meteor* cruises M29/2 and M46/3. This study has been conducted using E.U. Copernicus Marine Service Information, doi:10.48670/moi-00021. G. Kreps acknowledges support by the Open Access publication fund of Alfred-Wegener-Institut Helmholtz-Zentrum für Polar-und Meeresforschung. G. Kreps was supported by a fellowship from Deutscher Akademischer Austauschdienst (DAAD) under the founding program Research Grants—Bi-nationally Supervised Doctoral Degrees/Cotutelle (57552338). We thank Jürgen Titschack for his support with the grain-size measurements.

REFERENCES

Arhan, M., Heywood, K.J., and King, B.A., 1999, The deep waters from the Southern Ocean at the entry to the Argentine Basin: Deep Sea Research Part II, Topical Studies in Oceanography, v. 46, p. 475–499.

Artana, C., Ferrari, R., Koenig, Z., Sennéchael, N., Saraceno, M., Piola, A.R., and Provost, C., 2018a, Malvinas Current volume transport at 41 S: a 24 yearlong time series consistent with mooring data from 3 decades and satellite altimetry: Journal of Geophysical Research, Oceans, v. 123, p. 378–398.

Artana, C., Lellouche, J.M., Park, Y.H., Garric, G., Koenig, Z., Sennéchael, N., Ferrari, R., Piola, A.R., Saraceno, M., and Provost, C., 2018b, Fronts of the Malvinas Current System: surface and subsurface expressions revealed by satellite altimetry, Argo floats, and Mercator operational model outputs: Journal of Geophysical Research, Oceans, v. 123, p. 5261–5285.

Artana, C., Ferrari, R., Bricaud, C., Lellouche, J.M., Garric, G., Sennéchael, N., Lee, J.H., Park, Y.H., and Provost, C., 2021a, Twenty-five years of Mercator Ocean reanalysis GLORYS12 at Drake Passage: velocity assessment and total volume transport: Advances in Space Research, v. 68, p. 447–466.

Artana, C., Provost, C., Poli, L., Ferrari, R., and Lellouche, J.M., 2021b, Revisiting the Malvinas Current upper circulation and water masses using a high-resolution ocean reanalysis: Journal of Geophysical Research, Oceans, v. 126, e2021JC017271.

Artana, C., and Provost, C., 2023, Intense anticyclones at the global Argentine Basin array of the Ocean Observatory Initiative: Ocean Science, v. 19, p. 953–971.

Barré, N., Provost, C., and Saraceno, M., 2006, Spatial and temporal scales of the Brazil–Malvinas Current confluence documented by simultaneous MODIS Aqua 1.1-km resolution SST and color images: Advances in Space Research, v. 37, p. 770–786.

Bleil, U., 1994, Report and preliminary results of Meteor Cruise 29/2, Montevideo–Rio de Janeiro, 15.7.–8.8. 1994: Berichte, Fachbereich Geowissenschaften, Universität Bremen.

Bleil, U., 2001, Report and preliminary results of Meteor Cruise M 46/3, Montevideo–Mar del Plata, 04.01–07.02.2000: Berichte, Fachbereich Geowissenschaften, Universität Bremen.

Bleil, U., et al., 1993, Report and preliminary results of Meteor Cruise 23/2, Rio de Janeiro–Recife, 27.02.–19.03.1993: Berichte, Fachbereich Geowissenschaften, Universität Bremen.

Breitzke, M., Wiles, E., Krocker, R., Watkeys, M.K., and Jokat, W., 2017, Seafloor morphology in the Mozambique Channel: evidence for long-term persistent bottom-current flow and deep-reaching eddy activity: Marine Geophysical Research, v. 38, p. 241–269.

Buckley, M.W., and Marshall, J., 2016, Observations, inferences, and mechanisms of the Atlantic Meridional Overturning Circulation: a review: Reviews of Geophysics, v. 54, p. 5–63.

Buscaglia, J.L., 1971, On the circulation of the Intermediate Water in the southwestern Atlantic Ocean: Journal of Marine Research, v. 29, p. 245–255.

Cabanes, C., Grouazel, A., von Schuckmann, K., Hamon, M., Turpin, V., Coatanoan, C., Guinehut, S., Boone, C., Ferry, N., Reverdin, G., and Pouliquen, S., 2012, The CORA dataset: validation and diagnostics of ocean temperature and salinity in situ measurements: Ocean Science Discussions, v. 9, p. 1273–1312.

Chelton, D.B., Schlax, M.G., Samelson, R.M., and de Szoeke, R.A., 2007, Global observations of large oceanic eddies: Geophysical Research Letters, v. 95, p. 17,877–17,903.

Chidichimo, M.P., Perez, R.C., Speich, S., Kersalé, M., Sprintall, J., Dong, S., Lamont, T., Sato, O.T., Chereskin, T.K., Hummels, R., and Schmid, C., 2023, Energetic overturning flows, dynamic interocean exchanges, and ocean warming observed in the South Atlantic: Communications Earth & Environment, v. 4, no. 1.

Copernicus Marine Service, 2022, Global Ocean physics reanalysis: doi:10.48670/moi-00021.

Da Silveira, I.C.A., Calado, L., Castro, B.M., Cirano, M., Lima, J.A.M., and Mascarenhas, A.D.S., 2004, On the baroclinic structure of the Brazil Current: Intermediate Western Boundary Current system at 22–23S: Geophysical Research Letters, v. 31, p. 1–5.

de Miranda, A.P., Barnier, B., and Dewar, W.K., 1999, On the dynamics of the Zapiola Anticyclone: Journal of Geophysical Research, Oceans, v. 104, p. 21,137–21,149.

Ewing, M., and Lonardi, A.G., 1971, Sediment transport and distribution in the Argentine Basin. Sedimentary structure of the Argentine margin, basin, and related provinces: Physics and Chemistry of the Earth, v. 8, p. 125–251.

Faugères, J.C., Stow, D.A., Imbert, P., and Viana, A., 1999, Seismic features diagnostic of contourite drifts: Marine Geology, v. 162, p. 1–38.

Faugères, J.C., and Stow, D.A.V., 2008, Contourite drifts: nature, evolution and controls: Elsevier, Developments in Sedimentology, v. 60, p. 257–288.

Ferrari, R., and Wunsch, C., 2009, Ocean circulation kinetic energy: reservoirs, sources, and sinks: Annual Review of Fluid Mechanics, v. 41, p. 253–282.

Ferrari, R., Artana, C., Saraceno, M., Piola, A.R., and Provost, C., 2017, Satellite altimetry and current-meter velocities in the Malvinas Current at 41 S: comparisons and modes of variations: Journal of Geophysical Research, Oceans, v. 122, p. 9572–9590.

Fierens, R., Droz, L., Toucanne, S., Raisson, F., Jouet, G., Babonneau, N., and Jorry, S.J., 2019, Late Quaternary geomorphology and sedimentary processes in the Zambezi turbidite system (Mozambique Channel): Geomorphology, v. 334, p. 1–28.

Flood, R.D., 1988, A lee wave model for deep-sea mudwave activity: Deep Sea Research Part A, Oceanographic Research Papers, v. 35, p. 973–983.

Flood, R.D., and Shor, A.N., 1988, Mud waves in the Argentine Basin and their relationship to regional bottom circulation patterns: Deep Sea Research Part A, Oceanographic Research Papers, v. 35, p. 943–971.

Frenz, M., Höppner, R., Stuut, J.B.W., Wagner, T., and Henrich, R., 2004, Surface sediment bulk geochemistry and grain-size composition related to the oceanic circulation along the South American continental margin in the Southwest Atlantic, *in* Wefer, G., Mulitza, S., and Ratmeyer V., eds., The South Atlantic in the Late Quaternary: Reconstruction of Material Budgets and Current Systems: Berlin, Springer, p. 347–373.

Frey, D.I., Piola, A.R., and Morozov, E.G., 2023, Convergence of the Malvinas Current branches near 44° S: Deep Sea Research Part I, Oceanographic Research Papers, v. 196, no. 104023.

Fu, L.L., 2007, Interaction of mesoscale variability with large-scale waves in the Argentine Basin: Journal of Physical Oceanography, v. 37, p. 787–793.

Fu, L.L., Cheng, B., and Qiu, B., 2001, 25-day period large-scale oscillations in the Argentine Basin revealed by the TOPEX/Poseidon altimeter: Journal of Physical Oceanography, v. 31, p. 506–517.

Garzoli, S.L., and Garraffo, Z., 1989, Transports, frontal motions and eddies at the Brazil–Malvinas Currents Confluence: Deep Sea Research Part A, Oceanographic Research Papers, v. 36, p. 681–703.

Garzoli, S.L., Baringer, M.O., Dong, S., Perez, R.C., and Yao, Q., 2013, South Atlantic meridional fluxes: Deep Sea Research Part I, Oceanographic Research Papers, v. 71, p. 21–32.

GEBCO Compilation Group, 2023, GEBCO 2023: Grid, doi:10.5285/f98b053b-0cbc-6c23-e053-6c86abc0af7b.

Georgi, D.T., 1981, Circulation of bottom waters in the southwestern South Atlantic: Deep Sea Research Part A, Oceanographic Research Papers, v. 28, p. 959–979.

Gruetzner, J., Uenzelmann-Neben, G., and Franke, D., 2011, Variations in bottom water activity at the southern Argentine margin: indications from a seismic analysis of a continental slope terrace: Geo-Marine Letters, v. 31, p. 405–417.

Hernández-Molina, F.J., Llave, E., and Stow, D.A.V., 2008, Continental slope contourites: Elsevier, Developments in Sedimentology, v. 60, p. 379–408.

Hernández-Molina, F.J., Paterlini, M., Violante, R., Marshall, P., de Isasi, M., Somoza, L., and Rebesco, M., 2009, Contourite depositional system on the Argentine Slope: an exceptional record of the influence of Antarctic water masses: Geology, v. 37, p. 507–510.

Hernández-Molina, F.J., Paterlini, M., Somoza, L., Violante, R., Arecco, M.A., De Isasi, M., Rebesco, M., Uenzelmann-Neben, G., Neben, S., and Marshall, P., 2010, Giant mounded drifts in the Argentine Continental Margin: origins, and global implications for the history of thermohaline circulation: Marine and Petroleum Geology, v. 27, p. 1508–1530.

Hernández-Molina, F.J., Wåhlin, A., Bruno, M., Ercilla, G., Llave, E., Serra, N., and Sánchez-González, J.M., 2016, Oceanographic processes and morphosedimentary products along the Iberian margins: a new multidisciplinary approach: Marine Geology, v. 378, p. 127–156.

Hopfauf, V., and Spiess, V., 2001, A three dimensional theory for the development and migration of deep sea sedimentary waves: Deep-Sea Research Part I, Oceanography, v. 48, p. 2497–2519.

Kennett, J.P., 1983, Paleo-oceanography: global ocean evolution: Reviews of Geophysics, v. 21, p. 1258–1274.

Kolla, V., Eittreim, S., Sullivan, L., Kostecki, J.A., and Burckle, L.H., 1980, Current-controlled, abyssal microtopography and sedimentation in Mozambique Basin, southwest Indian Ocean: Elsevier, Marine Geology, v. 34, p. 171–206.

Kostov, Y., Armour, K.C., and Marshall, J., 2014, Impact of the Atlantic meridional overturning circulation on ocean heat storage and transient climate change: Geophysical Research Letters, v. 41, p. 2108–2116.

Kreps, G., Lembke-Jene, L., Romero, S., Ferrari, R., Lamy, F., and Miramontes, E., 2023, Bottom-current variability and the relationship with topography and sedimentary processes in the Drake Passage: Journal of Geophysical Research, Oceans, v. 128, e2022JC019623.

Ledbetter, M.T., 1986, Bottom-current pathways in the Argentine Basin revealed by mean silt particle size: Nature, v. 321, p. 423–425.

Ledbetter, M.T., and Johnson, D.A., 1976, Increased transport of Antarctic Bottom Water in the Vema Channel during the last ice age: Science, v. 194, p. 837–839.

Lellouche, J.M., Le Galloudec, O., Drévillon, M., Régnier, C., Greiner, E., Garric, G., Ferry, N., Desportes, C., Testut, C.E., Bricaud, C., and Bourdallé-Badie, R., 2013, Evaluation of global monitoring and forecasting systems at Mercator Océan: Ocean Science, v. 9, p. 57–81.

Lellouche, J.M., Greiner, E., Le Galloudec, O., Garric, G., Regnier, C., Drevillon, M., Benkiran, M., Testut, C.E., Bourdalle-Badie, R., Gasparin, F., and Hernandez, O., 2018, Recent updates to the Copernicus Marine Service global ocean monitoring and forecasting real-time 1/12° high-resolution system: Ocean Science, v. 14, p. 1093–1126.

Locarnini, M.M., Mishonov, A.V., Baranova, O.K., Boyer, T.P., Zweng, M.M., Garcia, H.E., Seidov, D., Weathers, K., Paver, C., and Smolyar, I., 2018, World Ocean Atlas 2018, Volume 1: Temperature: National Oceanic and Atmospheric Administration, v. 81, p. 1–52.

Lonardi, A.G., and Ewing, M., 1971, Sediment transport and distribution in the Argentine Basin. Bathymetry of the continental margin, Argentine Basin and other related provinces: canyons and sources of sediments: Physics and Chemistry of the Earth, v. 8, p. 81–121.

Lutjeharms, J.R.E., Meyer, A.A., Ansorge, I.J., Eagle, G.A., and Orren, M.J., 1996, The nutrient characteristics of the Agulhas Bank: South African Journal of Marine Science, v. 17, p. 253–274.

Lynn, R.J., and Reid, J.L., 1968, Characteristics and circulation of deep and abyssal waters [Abstract]: Elsevier, Deep Sea Research and Oceanographic Abstracts, v. 15, p. 577–598.

Madec, G., and the NEMO team, 2008, NEMO ocean engine, Note du Pole de modelisation: Institut Pierre-Simon Laplace, no. 1288-1619, p. 1–412.

Mata, M.M., Cirano, M., Caspel, M.R.V., Fonteles, C.S., Gǒni, G., and Baringer, M., 2012, Observations of Brazil Current baroclinic transport near 22 S: variability from the AX97 XBT transect: Clivar Exchanges, v. 17, p. 5–10.

Matano, R.P., Schlax, M.G., and Chelton, D.B., 1993, Seasonal variability in the southwestern Atlantic: Journal of Geophysical Research, Oceans, v. 98, p. 18027–18035.

McCave, I.N., and Hall, I.R., 2006, Size sorting in marine muds: processes, pitfalls, and prospects for paleoflow-speed proxies: Geochemistry, Geophysics, Geosystems, v. 7 p. 1–37.

McCave, I.N., and Swift, S.A., 1976, A physical model for the rate of deposition of fine-grained sediments in the deep sea: Geological Society of America, Bulletin, v. 87, p. 541–546.

McCave, I.N., Manighetti, B., and Robinson, S.G., 1995, Sortable silt and fine sediment size/composition slicing: parameters for palaeocurrent speed and palaeoceanography: Paleoceanography, v. 10, p. 593–610.

McCave, I.N., Thornalley, D.J.R., and Hall, I.R., 2017, Relation of sortable silt grain-size to deep-sea current speeds: calibration of the "Mud Current Meter": Deep Sea Research Part I, Oceanographic Research Papers, v. 127, p. 1–12.

Miramontes, E., Penven, P., Fierens, R., Droz, L., Toucanne, S., Jorry, S.J., Jouet, G., Pastor, L., Jacinto, R.S., Gaillot, A., and Giraudeau, J., 2019a, The influence of bottom currents on the Zambezi Valley morphology (Mozambique Channel, SW Indian Ocean): in situ current observations and hydrodynamic modelling: Marine Geology, v. 410, p. 42–55.

Miramontes, E., Garreau, P., Caillaud, M., Jouet, G., Pellen, R., Hernández-Molina, F. J., and Cattaneo, A., 2019b, Contourite distribution and bottom currents in the NW Mediterranean Sea: coupling seafloor geomorphology and hydrodynamic modelling: Geomorphology, v. 333, p. 43–60.

Miramontes, E., Jouet, G., Thereau, E., Bruno, M., Penven, P., Guerin, C., and Cattaneo, A., 2020, The impact of internal waves on upper continental slopes: insights from the Mozambican margin (southwest Indian Ocean): Earth Surface Processes and Landforms, v. 45, p. 1469–1482.

Miramontes, E., Thiéblemont, A., Babonneau, N., Penven, P., Raisson, F., Droz, L., Jorry, S.J., Fierens, R., Counts, J.W., Wilckens, H., and Cattaneo, A., 2021, Contourite and mixed turbidite–contourite systems in the Mozambique Channel (SW Indian Ocean): link between geometry, sediment characteristics and modelled bottom currents: Marine Geology, v. 437, no. 106502.

Miramontes, E., Kantner, R., Schwenk, T., and Kreps, G., 2024, Grain-distribution of surface sediments in the Argentine basin, R/V METEOR cruises M23-2, M29-2, M46-3 and M49-2: PANGAEA, doi:10.1594/PANGAEA.967514.

Mollenhauer, G., McManus, J.F., Benthien, A., Müller, P.J., and Eglinton, T.I., 2006, Rapid lateral particle transport in the Argentine Basin: molecular ^{14}C and ^{230}Thxs evidence: Deep Sea Research Part I, Oceanographic Research Papers, v. 53, p. 1224–1243.

Nielsen, T.A.P.M., Knutz, P.C., and Kuijpers, A., 2008, Seismic expression of contourite depositional systems: Elsevier, Developments in Sedimentology, v. 60, p. 301–321.

Olson, D.B., Podestá, G.P., Evans, R.H., and Brown, O.B., 1988, Temporal variations in the separation of Brazil and Malvinas Currents: Deep Sea Research Part A, Oceanographic Research Papers, v. 35, p. 1971–1990.

Orúe-Echevarría, D., Pelegrí, J.L., Machín, F., Hernández-Guerra, A., and Emelianov, M., 2019, Inverse modeling the Brazil–Malvinas confluence: Journal of Geophysical Research, Oceans, v. 124, p. 527–554.

Orúe-Echevarría, D., Polzin, K.L., Naveira Garabato, A.C., Forryan, A., and Pelegrí, J. L., 2023, Mixing and overturning across the Brazil–Malvinas confluence: Journal of Geophysical Research, Oceans, v. 128, e2022JC018730.

Paniagua, G.F., Saraceno, M., Piola, A.R., Guerrero, R., Provost, C., Ferrari, R., Lago, L.S., and Artana, C.I., 2018, Malvinas Current at 40 S–41 S: first assessment of temperature and salinity temporal variability: Journal of Geophysical Research, Oceans, v. 123, p. 5323–5340.

Park, Y.H., and Durand, I., 2019, Altimetry-Drived Antarctic Circumpolar Current Fronts: SEANOE, doi:10.17882/59800.

Park, Y.H., Park, T., Kim, T.W., Lee, S.H., Hong, C.S., Lee, J.H., Rio, M.H., Pujol, M.I., Ballarotta, M., Durand, I., and Provost, C., 2019, Observations of the Antarctic Circumpolar Current over the Udintsev Fracture Zone, the narrowest choke point in the Southern Ocean: Journal of Geophysical Research, Oceans, v. 124, p. 4511–4528.

Parker, G., Violante, A., and Paterlini, M.C., 1996, Fisiografía de la Plataforma Continental: Geología y Recursos Naturales de la Plataforma Continental Argentina, XIII Congreso Geológico Argentino y III Congreso de Exploración de Hidrocarburos, Buenos Aires, Asociación Geológica Argentina–Instituto Argentino del Petróleo, Relatorio, v. 1, p. 1–16.

Parker, G., Paterlini, M.C., and Violante, A., 1997, El fondo marino, in El Mar argentino y sus Recursos Marinos Pesqueros, 1: Mar del Plata, Instituto Nacional de Investigación y Desarrollo Pesquero, p. 65–87.

Pérez, F.F., Fontela, M., García-Ibáñez, M.I., Mercier, H., Velo, A., Lherminier, P., Zunino, P., de La Paz, M., Alonso-Pérez, F., Guallart, E.F., and Padin, X.A., 2018, Meridional overturning circulation conveys fast acidification to the deep Atlantic Ocean: Nature, v. 554, p. 515–518.

Pérez-Díaz, L., and Eagles, G., 2014, Constraining South Atlantic growth with seafloor spreading data: Tectonics, v. 33, p. 1848–1873.

Peterson, R.G., and Whitworth, T., III, 1989, The Subantarctic and Polar Fronts in relation to deep water masses through the southwestern Atlantic: Journal of Geophysical Research, Oceans, v. 94, p. 10,817–10,838.

Peterson, R.G., Johnson, C.S., Krauss, W., and Davis, R.E., 1996, Lagrangian Measurements in the Malvinas Current, *in* Wefer, G., Berger, W.H., Seidler, G., and Webb, D.J., eds., The South Atlantic: Present and Past Circulation: Springer, p. 239–247.

Petschick, R., Kuhn, G., and Gingele, F., 1996, Clay mineral distribution in surface sediments of the South Atlantic: sources, transport, and relation to oceanography: Marine Geology, v. 130, p. 203–229.

Piola, A.R., and Georgi, D.T., 1982, Circumpolar properties of Antarctic intermediate water and Subantarctic Mode Water: Deep Sea Research Part A, Oceanographic Research Papers, v. 29, p. 687–711.

Piola, A.R., and Gordon, A.L., 1989, Intermediate waters in the southwest South Atlantic: Deep Sea Research Part A, Oceanographic Research Papers, v. 36, p. 1–16.

Piola, A.R., and Matano, R.P., 2019, Ocean currents: Atlantic Western Boundary–Brazil Current/Falkland (Malvinas) Current, *in* Cochran, J.K., Bokuniewicz, H., and Yager, P., eds., Encyclopedia of Ocean Sciences, Third Edition: Elsevier, 4306 p.

Piola, A.R., Matano, R.P., Steele, J.H., Thorpe, S.A., and Turekian, K.K., 2001, Brazil and Falklands (Malvinas) currents: Ocean Currents, v. 1, p. 35–43.

Piola, A.R., Franco, B.C., Palma, E.D., and Saraceno, M., 2013, Multiple jets in the Malvinas Current: Journal of Geophysical Research, Oceans, v. 118, p. 2107–2117.

Poli, L., Artana, C., Provost, C., Sirven, J., and Le Blanc-Pressenda, R., 2024, Collapses, maxima, multi-year modulation and trends of the Zapiola Anticyclonic Circulation: insights from Mercator reanalysis: Journal of Geophysical Research, Oceans, v. 129, p.e2023JC020269.

Preu, B., Hernández-Molina, F.J., Violante, R., Piola, A.R., Paterlini, C.M., Schwenk, T., Voigt, I., Krastel, S., and Spiess, V., 2013, Morphosedimentary and hydrographic features of the northern Argentine margin: the interplay between erosive, depositional and gravitational processes and its conceptual implications: Deep Sea Research Part I, Oceanographic Research Papers, v. 75, p. 157–174.

Provost, C., and Le Traon, P.Y., 1993, Spatial and temporal scales in altimetric variability in the Brazil–Malvinas current confluence region: dominance of the semiannual period and large spatial scales: Journal of Geophysical Research, Oceans, v. 98, p. 18,037–18,051.

Pujol, M.I., Faugère, Y., Taburet, G., Dupuy, S., Pelloquin, C., Ablain, M., and Picot, N., 2016, DUACS DT2014: the new multi-mission altimeter data set reprocessed over 20 years: Ocean Science, v. 12, p. 1067–1090.

Purkey, S.G., Smethie, W.M., Jr., Gebbie, G., Gordon, A.L., Sonnerup, R.E., Warner, M. J., and Bullister, J.L., 2018, A synoptic view of the ventilation and circulation of Antarctic Bottom Water from chlorofluorocarbons and natural tracers: Annual Review of Marine Science, v. 10, p. 503–527.

Ramos, V.A. 1996, Evolución tectónica de la plataforma continental: Geología y recursos de la plataforma continental, *in* Ramos, V., and Turic, M., eds., Relatorio del XII Congreso Geológico Argentino y III Congreso de Exploración de Hidrocarburos, Asociación Geológica Argentina and Instituto Argentino de Petróleo y el Gas, p. 369–383.

Rebesco, M., and Camerlenghi, A., eds., 2008, Contourites: Elsevier, Developments in Sedimentology, v. 60, 653 p.

Rebesco, M., Hernández-Molina, F.J., Van Rooij, D., and Wåhlin, A., 2014, Contourites and associated sediments controlled by deep-water circulation processes: state-of-the-art and future considerations: Marine Geology, v. 352, p. 111–154.

Reid, J.L., and Nowlin, W.D., Jr., 1971, Transport of water through the Drake Passage [Abstract]: Elsevier, Deep Sea Research and Oceanographic Abstracts, v. 18, p. 51–64.

Reid, J.L., Nowlin, W.D., and Patzert, W.C., 1977, On the characteristics and circulation of the southwestern Atlantic Ocean: Journal of Physical Oceanography, v. 7, p. 62–91.

Rodrigues, S., Hernández-Molina, F.J., Larter, R.D., Rebesco, M., Hillenbrand, C.D., Lucchi, R.G., and Rodríguez-Tovar, F.J., 2022, Sedimentary model for mixed depositional systems along the Pacific margin of the Antarctic Peninsula: decoding the interplay of deep-water processes: Marine Geology, v. 445, no. 106754.

Saraceno, M., and Provost, C., 2012, On eddy polarity distribution in the southwestern Atlantic: Deep Sea Research Part I, Oceanographic Research Papers, v. 69, p. 62–69.

Saraceno, M., Provost, C., Piola, A.R., Bava, J., and Gagliardini, A., 2004, Brazil Malvinas Frontal System as seen from 9 years of advanced very high resolution radiometer data: Journal of Geophysical Research, Oceans, v. 109 no. C05027.

Saraceno, M., Provost, C., and Zajaczkovski, U., 2009, Long-term variation in the anticyclonic ocean circulation over the Zapiola Rise as observed by satellite altimetry: evidence of possible collapses: Deep Sea Research Part I, Oceanographic Research Papers, v. 56, p. 1077–1092.

Saunders, P.M., and King, B.A., 1995, Bottom currents derived from a shipborne ADCP on WOCE cruise A11 in the South Atlantic: Journal of Physical Oceanography, v. 25, p. 329–347.

Schmid, C., and Majumder, S., 2018, Transport variability of the Brazil Current from observations and a data assimilation model: Ocean Science, v. 14, p. 417–436.

Segl, M., 1994, Report and preliminary results of Meteor Cruise M29/1, Buenos Aires–Montevideo, 17.6.–13.7: Berichte, Fachbereich Geowissenschaften, Universität Bremen.

Solodoch, A., Stewart, A.L., and McWilliams, J.C., 2021, Formation of anticyclones above topographic depressions: Journal of Physical Oceanography, v. 51, p. 207–228.

Speer, K.G., and Zenk, W., 1993, The flow of Antarctic bottom water into the Brazil Basin: Journal of Physical Oceanography, v. 23, p. 2667–2682.

Spieß, V., 2002, Report and preliminary results of METEOR Cruise M 49/2, Montevideo (Uruguay)–Montevideo, 13.02.–07.03: Department of Geosciences, Bremen University.

Stow, D.A., Faugères, J.C., Howe, J.A., Pudsey, C.J., and Viana, A.R., 2002, Bottom currents, contourites and deep-sea sediment drifts: current state-of-the-art: Geological Society of London, Memoir 22, p. 7–20.

Stow, D.A., Hernández-Molina, F.J., Llave, E., Sayago-Gil, M., Diaz del Rio, V., and Branson, A., 2009, Bedform-velocity matrix: the estimation of bottom current velocity from bedform observations: Geology, v. 37, p. 327–330.

Stramma, L., and England, M., 1999, On the water masses and mean circulation of the South Atlantic Ocean: Journal of Geophysical Research, Oceans, v. 104, p. 20,863–20,883.

Straume, E.O., Gaina, C., Medvedev, S., Hochmuth, K., Gohl, K., Whittaker, J.M., Abdul Fattah, R., Doornenbal, J.C., and Hopper, J.R., 2019, GlobSed: updated total sediment thickness in the world's oceans: Geochemistry, Geophysics, Geosystems, v. 20, p. 1756–1772.

Szekely, T., Gourrion, J., Pouliquen, S., and Reverdin, G., 2019, The CORA 5.2 dataset for global in situ temperature and salinity measurements: data description and validation: Ocean Science, v. 15, p. 1601–1614.

Talley, L.D., 2003, Shallow, intermediate, and deep overturning components of the global heat budget: Journal of Physical Oceanography, v. 33, p. 530–560.

Thiéblemont, A., Hernández-Molina, F.J., Miramontes, E., Raisson, F., and Penven, P., 2019, Contourite depositional systems along the Mozambique channel: the interplay between bottom currents and sedimentary processes: Deep Sea Research Part I, Oceanographic Research Papers, v. 147, p. 79–99.

Thran, A.C., Dutkiewicz, A., Spence, P., and Müller, R.D., 2018, Controls on the global distribution of contourite drifts: insights from an eddy-resolving ocean model: Earth and Planetary Science Letters, v. 489, p. 228–240.

Trenberth, K.E., and Zhang, Y., 2019, Observed interhemispheric meridional heat transports and the role of the Indonesian throughflow in the Pacific Ocean: Journal of Climate, v. 32, p. 8523–8536.

Urien, C.M., and Zambrano, J.J., 1996, Estructura del Margen Continental: Geología y recursos de la plataforma continental, *in* Ramos, V., and Turic, M., eds., Relatorio del XII Congreso Geológico Argentino y III Congreso de Exploración de Hidrocarburos, Asociación Geológica Argentina and Instituto Argentino de Petróleo y el Gas, p. 29–65.

Valla, D., Piola, A.R., Meinen, C.S., and Campos, E., 2018, Strong mixing and recirculation in the northwestern Argentine Basin: Journal of Geophysical Research, Oceans, v. 123, p. 4624–4648.

Van Andel, T.H., Thiede, J., Sclater, J.G., and Hay, W.W., 1977, Depositional history of the South Atlantic Ocean during the last 125 million years: The Journal of Geology, v. 85, p. 651–698.

Vivier, F., and Provost, C., 1999, Direct velocity measurements in the Malvinas Current: Journal of Geophysical Research, Oceans, v. 104, p. 21,083–21,103.

von Lom-Keil, H., Spieß, V., and Hopfauf, V., 2002, Fine-grained sediment waves on the western flank of the Zapiola Drift, Argentine Basin: evidence for variations in Late Quaternary bottom flow activity: Marine Geology, v. 192, p. 239–258.

Weatherly, G.L., 1993, On deep-current and hydrographic observations from a mudwave region and elsewhere in the Argentine Basin: Deep Sea Research Part II, Topical Studies in Oceanography, v. 40, p. 939–961.

Wefer, G., Berger, W.H., Siedler, G., Webb, D.J., and Talley, L.D., 1996, Antarctic intermediate water in the South Atlantic, *in* Wefer, G., Berger, W.H., Seidler, G., and Webb, D.J., eds., The South Atlantic: Present and Past Circulation: Springer, p. 219–238.

Wilckens, H., Miramontes, E., Schwenk, T., Artana, C., Zhang, W., Piola, A.R., Baques, M., Provost, C., Hernández-Molina, F.J., Felgendreher, M., and Spieß, V., 2021, The erosive power of the Malvinas Current: influence of bottom currents on morpho-sedimentary features along the northern Argentine margin (SW Atlantic Ocean): Marine Geology, v. 439, no. 106539.

Wright, W.R., 1970, Northward transport of Antarctic bottom water in the western Atlantic Ocean [Abstract]: Elsevier, Deep Sea Research and Oceanographic Abstracts, v. 17, p. 367–371.

Zhao, Y., Liu, Z., Zhang, Y., Zhang, X., Ma, P., Yu, X., and Zhang, J., 2024, Formation mechanism of drift-moat contourite systems revealed by in-situ observations in the South China Sea: Earth and Planetary Science Letters, v. 628, no. 118585.

Zweng, M.M., Seidov, D., Boyer, T.P., Locarnini, M., Garcia, H.E., Mishonov, A.V., Baranova, O.K., Weathers, K., Paver, C.R., and Smolyar, I., 2019, World Ocean Atlas 2018, Volume 2: Salinity: National Oceanic and Atmospheric Administration, v. 82, p. 1–50.

Received 18 January 2024; accepted 30 June 2024.